RSC Applied Polymers

PAPER

View Article Online
View Journal | View Issue

Cite this: *RSC Appl. Polym.*, 2025, **3**, 1545

Scorpion-inspired transparent, antibacterial, UV shielding, and self-healing fluorescence polymer materials

Wenjin Wu,[a] Jie Dong,[a] Yingxin Shen,[a] Yijia Yang,[a] Yingliang Wu,*[b] Xiaojuan Liao *[a] and Kun Huang *[a]

Received 4th July 2025,
Accepted 1st September 2025

DOI: 10.1039/d5lp00203f

rsc.li/rscapplpolym

As ancient Earth creatures, scorpions have adapted well to various complex living environments after hundreds of millions of years of biological evolution. Their exoskeleton (cuticle) emits blue-green bioluminescence under UV radiation. This paper studies the synthesis and properties of poly(butyl acrylate-*co*-*N*-isopropylacrylamide) (PBN-MDE) film doped with the scorpion's fluorescent molecule macrocyclic diphthalate ester (MDE). The MDE fluorescent molecules can form dynamic hydrogen bonds with the PBN polymer chain, greatly enhancing its mechanical properties, with specific ductility and toughness nearly ten times before doping. In addition, the PBN-MDE film not only has excellent visible light transmittance and can display obvious fluorescence under UV light (365 nm), but also exhibits preeminent UV shielding efficiency (<400 nm) and good bacteriostatic activity for Gram-positive bacteria and Gram-negative bacteria. These special functions of the PBN-MDE film can effectively extend its service life and are expected to achieve UV-resistant coatings with functions such as information protection, adaptive camouflage, or information transmission.

1. Introduction

Many animals or plants in nature can emit biological fluorescence under environmental stimuli, which is caused by the absorption of electromagnetic radiation such as high-energy blue light or ultraviolet radiation.[1–3] This biological fluorescence generally has specific functions, such as killing prey, fending off predators, attracting mates, and more.[4,5] Inspired by these bioluminescence phenomena and their distinctive functions, there have been many cases in which stimuli-responsive fluorescence phenomena have been successfully applied to polymer materials with various functions.[6–8] Inspired by Noctiluca scintillans, Yin and co-workers realized a new type of optical material with an illusionary emission phenomenon of fluorescence located at a long wavelength but displaying the afterglow with a short wavelength, through precise modulation of ultralong organic phosphorescence (UOP). This dual-mode information encryption can effectively solve common problems such as information leakage and counterfeiting.[9] Inspired by chameleons, Liu *et al.* developed a multi-color fluorescent polymer material, which was used as adaptive color-changing bionic skin to enable dynamic camouflage for soft robots.[10] Flexible polymer materials in combination with biological fluorescence are not only commonly used for information encryption,[11,12] camouflage, and display of soft robots in the environment,[13–15] but can also be applied to nano-bionic sensors.[16,17] Leveraging the natural ability of wild-type plants to pre-concentrate and extract arsenic from the belowground environment, Lew and co-workers designed a pair of single-walled carbon nanotube (SWNT)-based near-infrared (NIR) fluorescent nanosensors to selectively recognize arsenite *via* modulation of their emission intensity.[18]

Most scorpions exhibit an interesting characteristic, whereby their exoskeleton (cuticle) emits blue-green fluorescence in the 420–650 nm range when exposed to UV radiation (315–400 nm),[19] although different species of scorpions have different adaptive functions to the environment in which they live. There are many hypotheses about the biological functions of the scorpion cuticle fluorescence, but the functionality of this interesting biological fluorescence (if any) is still unclear.[20,21] Various fluorescent substances have been isolated from scorpion molting.[22–24] However, it is still rare to utilize this biological fluorescence for the functionalization and investigation of polymer materials. In our previous report, we modified the scorpion natural fluorescent molecule macrocyclic diphthalate ester (MDE) into divinyl macrocyclic

[a]*School of Chemistry and Molecular Engineering, East China Normal University, Shanghai, 200241, China. E-mail: xjliao@chem.ecnu.edu.cn, khuang@chem.ecnu.edu.cn*
[b]*College of Life Sciences, Wuhan University, Wuhan, 430072, China. E-mail: ylwu@whu.edu.cn*

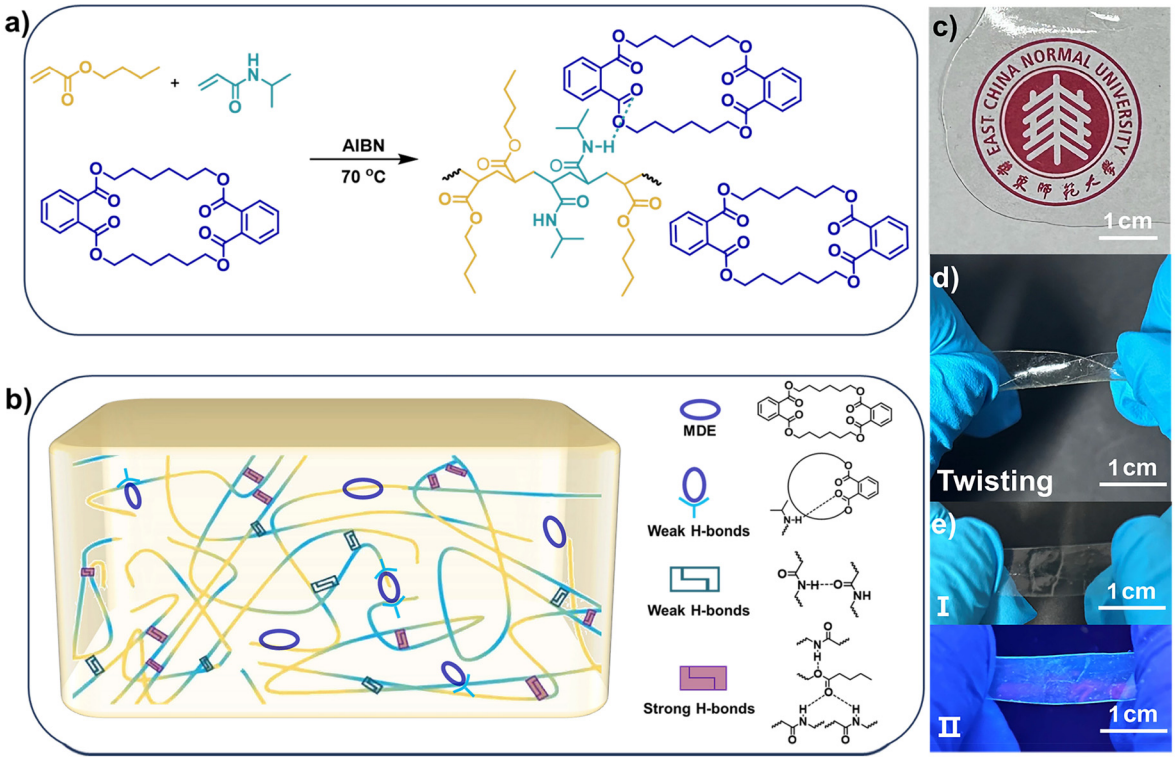

Scheme 1 Synthesis of scorpion-inspired fluorescent polymers PBN-MDE. (a) Synthesis of self-healing PBN-MDE elastomers. (b) Schematic illustration of the polymer structure in PBN-MDE. Optical images of (c) light transmittance, (d) flexibility, and (e) fluorescence under UV light of PBN-MDE.

diphthalate ester (DVMDE) as a crosslinking agent to prepare a fluorescent anti-counterfeiting coating with excellent optical transparency, and it was also demonstrated that the polymer films containing DVMDE had a broad-spectrum antimicrobial effect against Gram-positive bacteria.[25]

Inspired by the scorpion's ability to collect light energy and convert it into fluorescent information, we directly doped the scorpion natural product MDE to prepare transparent self-repairing fluorescent polymer materials with information encryption coating with UV shielding and antibacterial effects, which mimicked the fluorescent function of scorpions based on our previous work. Specifically, we introduced the MDE functional molecules directly into the *in situ* polymerization network of butyl acrylate (BA) and *N*-isopropylacrylamide (NIPAM) to obtain a uniformly textured transparent film PBN-MDE (Scheme 1). The film doped with the scorpion's fluorescent molecule MDE not only retains the mechanical strength of the PBN film formed by poly(butyl acrylate-*co*-*N*-isopropylacrylamide), but also greatly improves ductility. Among them, the strain at break of PBN-MDE increases greatly from 39% to 400%, and the toughness increases from 0.3 MJ m^{-3} to 28.9 MJ m^{-3}. Moreover, the fluorescence intensity of the PBN-MDE films is significantly enhanced under the excitation of λ = 270 nm.

This newly prepared PBN-MDE film also has excellent UV shielding ability. When the doping amount of MDE reaches 30 wt%, the shielding rate of UV-A2 (315–340 nm) can reach 100%, and the shielding rate of UV-A1 (340–400 nm) can reach 78%. It is very important for the durability of the coating that the PBN-MDE film has excellent self-healing ability at 40 °C and can be recycled after recovery. In addition, the PBN-MDE film exhibits good light transmittance in the visible light range and demonstrates excellent antibacterial effects against Gram-positive bacteria, making the coating show great application potential in biomedicine.

2. Results and discussion

Materials design and synthesis of PBN-MDE

Macrocyclic diphthalate ester (MDE) from scorpion molting can produce a strong blue-green fluorescence under irradiation of a 365 nm UV light. To extend the functionality of this fluorescent compound, we introduced MDE into the PBN polymer film using the simplest doping method. Specifically, to ensure uniform distribution of the MDE compound in the polymer system, we added MDE and *N*-isopropylacrylamide (NIPAM) to a 10 mL round-bottom flask under a nitrogen atmosphere to be dissolved in 1,4-dioxane solvent. Then, butyl acrylate (BA) and *azo*-diisobutyl nitrile (AIBN) were added in sequence, and the reaction was carried out at 70 °C for 24 hours with thorough stirring to ensure the uniform distribution of the dopant. After the reaction was complete, the prepolymer was

transferred to a polytetrafluoroethylene (PTFE) mold and cured. After demolding, the obtained transparent polymer films were named PBN-MDE-*X* (*X* wt% MDE, *X* = 5, 10, 15, 20, 25, 30) according to the amount of doping MDE (the amount of MDE doping is the percentage of the mass of BA and NIPAM). The preparation process of PBN film is similar to that of PBN-MDE film without MDE.

Materials characterizations of PBN-MDE and PBN films

The ^{1}H NMR spectra of the prepared PBN and PBN-MDE polymers are shown in Fig. 1a. Comparing the ^{1}H NMR of BA, NIPAM, PBN, and PBN-MDE, it is evident that the peaks attributed to the vinyl groups of BA and NIPAM have completely disappeared in both PBN and PBN-MDE, indicating that the polymerization between BA and NIPAM is complete. Simultaneously, the hydrogen atoms belonging to the amide bond in PBN have significantly shifted compared to those in the NIPAM monomer, indicating the presence of hydrogen bonds in the PBN polymer. The hydrogen atoms on the amide bond in PBN-MDE have also shifted significantly compared with those in PBN and the NIPAM monomer. Through gel permeation chromatography (GPC) testing, it was found that the molecular weight of the PBN-MDE-20 polymer has significantly increased compared to PBN (Fig. S4 and S5). These results suggest that, in addition to the ability to generate physical entanglement within the polymer network, the formation of dynamic hydrogen bonds with hydrogen atoms on amide groups further promotes chemical crosslinking between chains through the doping of MDE.[26] This conclusion was also confirmed in the FT-IR spectra. As shown in Fig. 1b, the bending vibration of the monosubstituted olefin –CH=CH$_2$, which was observed at 991 cm^{-1}, disappeared, and the newly formed bending vibration of the *trans*–CH$_2$–CH– at the –C–H– bond appeared at 960 cm^{-1}. These observations clearly suggest that the radical polymerization has been substantially completed. As can be seen from locally magnified Fig. 1c and d, the stretching vibration attributed to the ester bond C=O at 1730 cm^{-1} shows an obvious blue-shift with the increasing MDE doping amount. At the same time, the characteristic peak of the amide group at 1260 cm^{-1} is also red-shifted obviously, and the vibrational band is widened with the doping of MDE.[27] All of the observations indicate that the dynamic hydrogen bond was formed in PBA-MDE after MDE was added.

The TGA curves of PBN and PBN-MDE were analyzed for thermal weight loss (Fig. S6a). It was observed that the polymers exhibit higher thermal stability with thermal decomposition temperatures above 300 °C. The doping of MDE did not significantly affect the thermal stability of the polymers, which makes them suitable for operation in a high-temperature environment. Fig. S6b showed the differential scanning calorimetry (DSC) curves of PBN and PBN-MDE. The glass transition temperature (T_g) of PBN is 52 °C, indicating little elasticity and strong rigidity under room temperature conditions. With the increase in MDE doping amount, the T_g of PBN-MDE decreases significantly, and the polymer chain gradually tends to be flexible. This is due to the decreased cross-linking degree of polymer molecules after MDE doping, which facilitates molecular chain movement, improving the flexibility of the material and reducing the T_g. Among them, the T_g of PBN-MDE-20 and PBN-MDE-30 was 23 °C and 17 °C, respectively, which exhibit good flexibility under room temperature conditions.

Mechanical properties of PBN-MDE and PBN films

In this work, the mechanical properties of the PBN polymer were improved by doping the scorpion's fluorescent molecule MDE into the PBN polymer. As shown in Fig. 2a, the appropriate mechanical properties of the PBN films were firstly obtained by adjusting the molar ratio of BA and NIPAM. The synthesized PBN polymers were named as PBN-4 : 6 (BA : NIPAM = 4 : 6), PBN-1 : 1 (BA : NIPAM = 1 : 1), and PBN-6 : 4 (BA : NIPAM = 6 : 4) according to the different molar ratios of BA and NIPAM. The prepared PBN-1 : 1 film had a high tensile strength of 16.1 MPa, but the elongation at break was less than 40%. When the molar ratio of BA and NIPAM is 4 : 6, the elongation at break of the PBN-4 : 6 film is 192%, and the tensile strength is only 9.3 MPa. When the molar ratio of

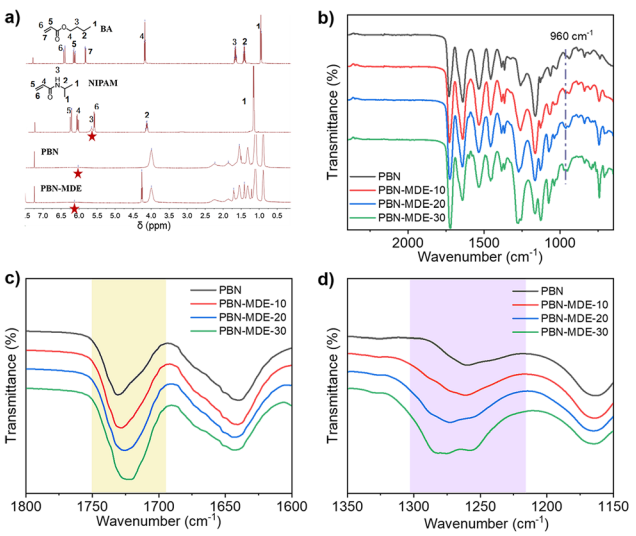

Fig. 1 Structural characterizations of PBN and PBN-MDE. (a) ^{1}H NMR and (b), (c), and (d) FT-IR spectra at room temperature.

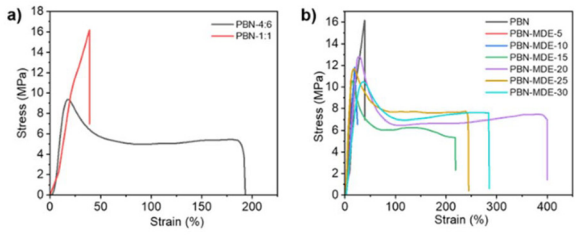

Fig. 2 Stress–strain curves of PBN with different molar ratios of BA and NIPAM (a) and PBN-MDE with different doping amounts of MDE (b).

BA and NIPAM is 6 : 4, the cured PBN-6 : 4 film is brittle and difficult to completely peel from the PTFE mold. It is considered that after doping rigid small molecule compounds in PBN, the crosslinking degree of the polymer is reduced and the flexibility is enhanced. In order to minimize the negative impact of doping MDE on the mechanical strength of the material, the relatively rigid PBN-1 : 1 was selected as the template for doping. The effect of doping MDE with different weight ratios on the mechanical properties of the polymer is shown in Fig. 2b. When the doping amount of MDE was 5 wt%, the tensile strength of the polymer decreased significantly, and it still maintained rigidity overall. When the MDE doping was 10 wt%, the mechanical properties of the polymer were enhanced slightly compared with PBN-MDE-5 (tensile strength from 10.5 MPa to 11.9 MPa, and elongation at break from 11.5% to 19.0%). There is not a significant effect of low doping amounts on the mechanical properties of the polymer. However, when the doping amount of MDE was 15 wt%, the polymer transformed from rigid to plastic deformation with no significantly changed tensile strength, but the strain increased to 217%. When the doping amount of MDE was greater than 20 wt%, the tensile strength of the polymer decreased overall, and the elongation at break also began to decrease significantly. This may be due to the fact that 20 wt% MDE is better balanced in the polymer system through physical entanglement or non-covalent bonding, such as hydrogen bonding with the polymer chains. Therefore, the PBN-MDE-20 film, which exhibits the tensile strength (12.8 MPa), elongation at break (400%), and toughness (28.9 MJ m^{-3}), was selected as the experimental template for further exploration of the polymer's functionality.

The self-healing and recyclability of PBN-MDE

In order to study the self-healing properties of PBN-MDE films, the PBN-MDE-20 film with excellent mechanical properties was used as a typical sample. It was cut in the middle with a sharp blade at room temperature, and the cut surfaces were then brought into contact again for more than 12 hours. The cut marks were still evident, and the mechanical strength had not been restored, making it unsuitable for tensile testing. However, when the temperature was raised to 40 °C, and the cut surfaces were kept in contact for 2 hours, the cut mark of the PBN-MDE-20 film disappeared (Fig. 3d–f). The tensile test was conducted after cooling to room temperature (Fig. 3a), and the stress–strain curve after healing was found to be almost consistent with that before healing. This is attributed to the presence of dynamic hydrogen bonds and entanglement of molecular chains in PBN-MDE-20. The dynamic hydrogen bonds reassociate, and the molecular chain motion is accelerated, enabling self-healing of the polymer in the heating environment. As shown in Fig. 3b and c, the tensile strength of the healed PBN-MDE-20 film was 13.3 MPa with a tensile strength self-healing efficiency of 103%. The elongation at break was 372% with an elongation at break self-healing efficiency of 93%. The toughness was 30.6 MJ m^{-3}, with a toughness self-healing efficiency of 106%. The self-healing efficiency for tensile strength and toughness greater than 100% was caused by mechanical errors in the test or hydrogen bond rearrangement to achieve equilibrium during heating.[28–31]

Due to the need for sustainable development, the recycling of novel materials is a crucial consideration. Depolymerizing

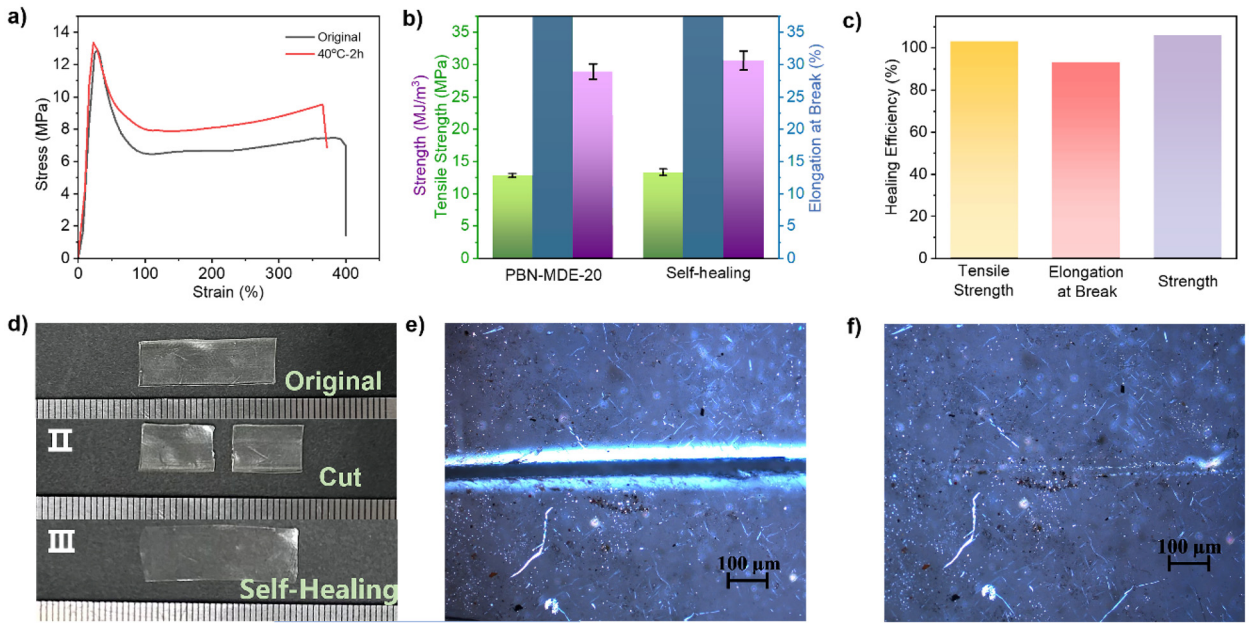

Fig. 3 Self-healing behavior of PBN-MDE-20. (a) Stress–strain curves before and after self-healing. (b) The bar graph of toughness, tensile strength, and elongation break. (c) The bar graph of self-healing efficiency. (d) Images of the surface-damaged sample and healed sample at 40 °C. (e and f) Optical microscope images of the damaged state (e) of film and the healed state (f) after 2 h (scale bar: 100 μm).

materials into monomers or oligomers and then re-polymerizing them is a promising strategy for material recovery.[32,33] PBN and PBN-MDE-20 films are easily dissolved in dichloromethane to form a clear and homogeneous polymer solution. During the process of removing the organic solvent, the disrupted non-covalent interactions and linear chain entanglement can be reestablished, restoring the original state of the polymer film.[34] With this performance, PBN and PBN-MDE-20 films can realize recycling after recovery. As shown in Fig. 4a and b, the polymer films of PBN and PBN-MDE-20 were cut into pieces, then dissolved in a small amount of dichloromethane for 30 minutes and transferred to a PTFE mold to achieve recycling by heating. The mechanical properties of the recycled samples PBN-Recycle and PBN-MDE-20-Recycle films were tested. The stress–strain curves are shown in Fig. 4c, and the recycled tensile curves almost overlap with the original curves. Based on calculations (Fig. 4d), the recycling efficiency of the PBN-Recycle film is nearly 100%, and the recycling efficiency of the PBN-MDE-20-Recycle film is more than 90%. The mechanical properties of the MDE-doped PBN-MDE-20 film did not decrease significantly after recycling, and the recycling efficiency did not decrease notably compared to the PBN film. Doping MDE can enhance the mechanical properties of the polymer film while having a negligible effect on its recyclability, due to the re-form entanglement and non-covalent interactions between the polymer's linear chains during the evaporation of organic solvents. The self-healing of PBN-MDE films is highly desirable for the durability of coatings used in long-term applications, and the solution recovery facilitates the preparation of various shapes, enabling them to meet diverse application scenarios and functional requirements.[35]

Fluorescence property and UV resistance of PBN-MDE

The scorpion's fluorescent compound MDE can be used as a natural fluorescent dye because of its obvious fluorescence phenomenon under 365 nm UV radiation. The MDE was doped in the PBN film, and the fluorescence emission spectrum of a 0.2 mm-thick film was tested using an excitation wavelength of 270 nm (Fig. 5a). The fluorescence spectrum of the PBN polymer film has two obvious fluorescence emission peaks at 450–550 nm and 600–770 nm, which may be caused by the energy transfer between heteroatoms such as nitrogen, oxygen, and carbonyl groups promoted by hydrogen bonding aggregation, resulting in fluorescence excitation in the visible region.[36] When doped with MDE, the fluorescence of PBN-MDE-20 film was significantly enhanced in the range of 550–800 nm. At the same time, the fluorescence intensity of PBN-MDE-20 visible to the unaided eye was higher under the irradiation of 365 nm UV light, which was consistent with the fluorescence spectra test results (Fig. 5b). The photoluminescence behavior of the PBN-MDE coating was stable during stretching (Fig. S7). As shown in Fig. 5c and d, the PBN-MDE-20 prepolymer solution was transferred and printed onto different materials through a heart-shaped template, followed by solvent evaporation. The heart-shaped pattern on different materials was not clear under natural light, but it becomes visible due to fluorescence when illuminated by a 365 nm UV light. The fluorescent property of optically transparent PBN-MDE-20 film has the potential to be used as a coating for information transmission or anti-counterfeiting, which provides new possibilities for addressing threats to personal and economic security caused by information leaks.

UV-resistant polymer materials are widely used in high-end clothing, packaging materials, smart coatings, and other fields. The UV transmission spectra of PBN-MDE and PBN

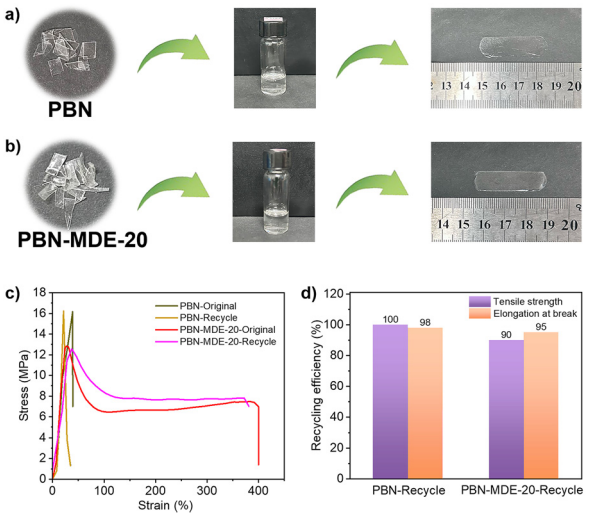

Fig. 4 Recycling properties of PBN and PBN-MDE-20 polymer. (a) and (b) Recycling study. The PBN (a) and PBN-MDE-20 (b) films were cut and dissolved in DCM, and the recovered films were obtained by drying the organic solvent. (c) Stress–strain curves of PBN and PBN-MDE-20 before and after recovery. (d) The bar graph of recovery efficiency of PBN and PBN-MDE-20 films.

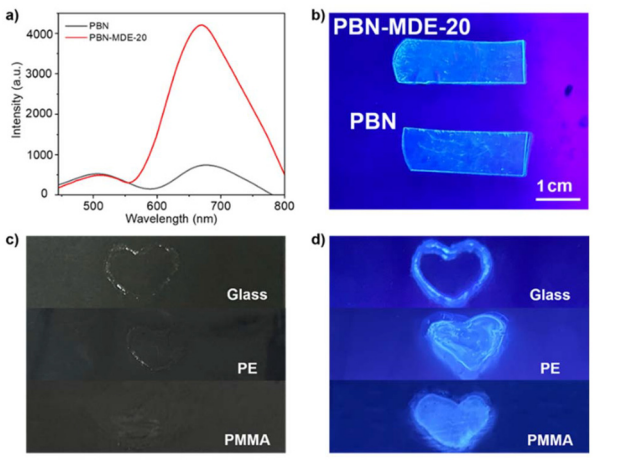

Fig. 5 Fluorescence properties. (a) Fluorescence spectra of the films of PBN and PBN-MDE-20 with light excitation at 270 nm (thickness, 0.2 mm). (b) Comparison of fluorescence images of PBN and PBN-MDE-20 film excited by UV light of 365 nm. Digital images of heart-shaped patterns in different materials, exposed to natural light (c) and UV light of 365 nm (d).

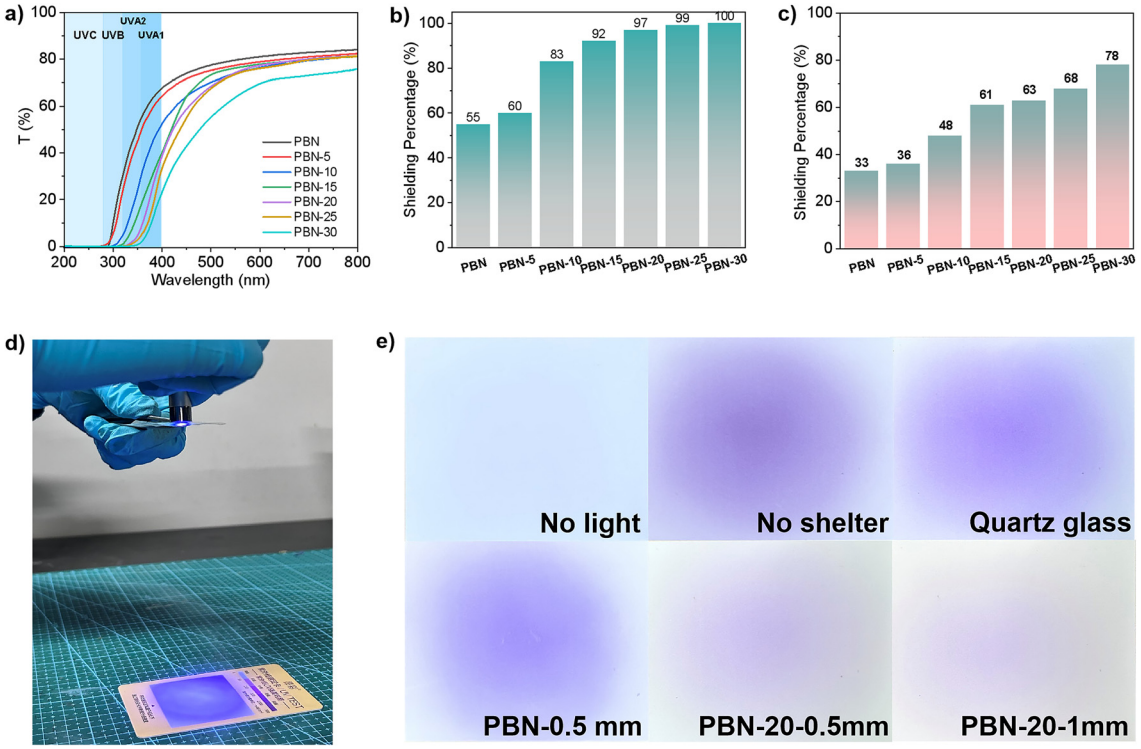

Fig. 6 (a) Ultraviolet transmission spectra of a series of PBN and PBN-MDE films (thickness of 0.5 mm). (b) Shielding percentage at 340 nm for PBN and PBN-MDE films. (c) Shielding percentage at 400 nm for PBN and PBN-MDE films. (d) Experimental demonstration of the UV light beam irradiating the UV test card. (e) Photos of the UV light beam irradiating the UV test card under different conditions.

films (0.5 mm thick) are shown in Fig. 6a. All the films had excellent optical transparency with transmittance of over 80%, except for PBN-MDE-30. At the same time, the UV transmittance of all films in the UV-C (<280 nm) was 0. Polymer films doped with 15 wt% or more MDE exhibited a UV transmittance of 0% in the UV-B (280–315 nm). The PBN-MDE-20, PBN-MDE-25, and PBN-MDE-30 films had a UV transmittance that was almost 0% in the UV-A2 (315–340 nm). Furthermore, the shielding efficiency of PBN-MDE-30 was 78% in the UV-A1 (340–400 nm). Overall, the UV shielding of PBN-MDE-20, PBN-MDE-25, and PBN-MDE-30 films demonstrated nearly 100% in the near-UV (200–380 nm). As shown in Fig. 6b and c, the UV shielding of the PBN-MDE films significantly increases with the increase in the doping amount of MDE. Although the doping amount of MDE plays an indispensable role in the UV shielding of the polymer films, too high a doping amount (≥30 wt%) can reduce the transparency of the polymer films and result in a decrease in visible light transmittance.

To further investigate the practical application of UV resistance of the films, considering their mechanical properties, transmittance, and UV shielding, we took PBN-MDE-20 as an example. As demonstrated in Fig. 6d, a handheld violet-full-spectrum lamp was used to irradiate the polymer film surface with UV light for 5 seconds (the handheld light was in direct contact with the film, and the distance between the film and the UV test card was 15 cm). The UV test card presented different shades of purple based on the UV shielding of the material, allowing us to judge the intensity of UV radiation. As shown in Fig. 6e, quartz glass was used as a control group, and the feasibility of the test experiment was verified by comparing the colors of the UV test card in the absence of light and direct radiation. The test results showed that quartz glass had almost no UV shielding. The PBN film with a thickness of 0.5 mm exhibited weak UV shielding, while the same thickness of PBN-MDE-20 significantly enhanced UV blocking, resulting in a very light purple color on the test card. It is further confirmed that MDE is an effective component for UV shielding in PBN-MDE films. When the thickness of the PBN-MDE-20 film increased to 1 mm, the color of the UV test card became significantly lighter compared to that of the PBN-MDE-20 film at 0.5 mm, which was nearly colorless. Therefore, increasing the thickness of the PBN-MDE films can effectively improve their UV shielding efficiency. As is well known, high-energy UV light in sunlight is the main cause of material photodegradation and photoaging. The PBN-MDE-20 film not only has high transparency but also shows effective blockage of UV radiation. Therefore, its potential expansion into a wider range of practical applications to address UV photodegradation and performance degradation issues is suggested.

Antibacterial properties of PBN-MDE films

As the stratum corneum is the first line of defence in arthropods, the extract MDE from scorpion molting may play a role in preventing parasitic infections. Existing studies have shown that the

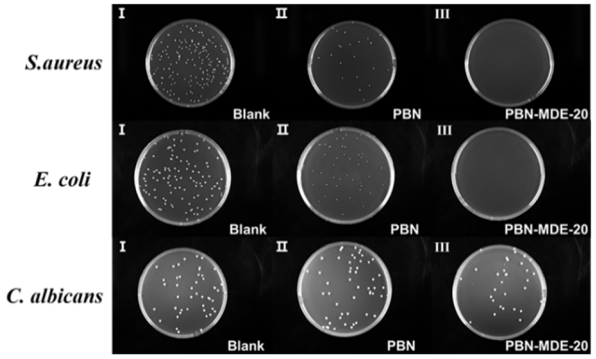

Fig. 7 Photographs of colonies after colony co-culture with *S. aureus*, *E. coli*, *C. albicans*: (I) blank, (II) PBN, (III) PBN-MDE-20.

Table 1 Antimicrobial activity of PBN and PBN-MDE-20 against *S. aureus*, *E. coli*, *C. albicans* evaluated by counting colonies on agar plates

Antimicrobial rate (%)	PBN	PBN-MDE-20
S. aureus	85	>99.9
E. coli	54	>99.9
C. albicans	—	27.9%

MDE compound exhibits anti-Leishmania, antifungal, and anti-Gram-positive bacterial activities.[24,25] To verify whether PBN-MDE has inhibitory effects on Gram-positive bacteria, Gram-negative bacteria, and fungi, the antibacterial activity of PBN and PBN-MDE-20 was tested using the plate spread method. *Staphylococcus aureus*, *Escherichia coli*, and *Candida albicans* were selected for testing because they are common Gram-positive, negative, and fungal pathogens in life. As shown in Fig. 7, the bacterial solution was dropped on the surface of the film and cultured for 24 hours before being diluted and counted for colony formation. Compared to the control group, both PBN and PBN-MDE-20 showed significant antibacterial effects. The antimicrobial rates against *S. aureus* and *E. coli* were 85% and 54% for PBN, while they were 100% and 100% for PBN-MDE-20 (Table 1). Although PBN also exhibits good antibacterial activity, the addition of the MDE compound enhanced the antibacterial rate to 100%. MDE exhibits inhibitory activity against Gram-positive bacteria, Gram-negative bacteria, and fungi. The prepared PBN-MDE films can effectively inhibit microbial growth and reduce the biological toxicity of the material, thereby prolonging the service life of the coating, which provides a new choice for biomedical materials.[37]

3. Conclusions

Inspired by the fluorescence of scorpions, we successfully prepared a self-healing fluorescent polymer, PBN-MDE, that effectively shields UV radiation by simply doping with MDE. The ~0.5 mm-thick PBN-MDE film delivers broadband UV shielding (>80% attenuation of UVA/UVB/UVC), offering great potential for protecting underlying substrates and human skin and extending the service life of outdoor electronics, photovoltaic panels, and wearable sensors. Furthermore, the PBN-MDE film, which maintains high transparency and resolution under natural light, also exhibits markedly improved mechanical properties, achieves nearly 100% self-healing efficiency at 40 °C, retains its mechanical integrity after solution recycling, shows significantly intensified fluorescence under 365 nm UV light, and effectively inhibits both Gram-positive and Gram-negative bacteria. In summary, we have replicated the fluorescent behavior of scorpions to prepare a multifunctional bionic film exhibiting excellent mechanical properties, which provides a new possibility for prolonging the coating life and realizing a UV shielding coating with information encryption technology.

Author contributions

Yingliang Wu, Xiaojuan Liao, Kun Huang, and Wenjin Wu conceived the concept and edited the manuscript. Each author contributed expertise to write the following sections: Wenjin Wu completed the main synthesis as well as the test analysis, Jie Dong purified the synthesized product, Yingxin Shen and Yijia Yang participated in the design of the experimental design for UV shielding, and Yingliang Wu provided support for antibacterial experiments. All authors provided feedback and approved the manuscript for submission.

Conflicts of interest

There are no conflicts to declare.

Data availability

The authors declare that the data supporting the findings of this study are available within the paper and its SI files. Supplementary information: additional experimental details, NMR spectra of intermediate and monomer, cyclic tensile testing, TGA curves and FT-IR of polymer (DOC). See DOI: https://doi.org/10.1039/d5lp00203f.

Acknowledgements

All authors acknowledge the support of the National Natural Science Foundation of China (22375064, 32170519).

References

1 G. Lee, M. Kong, D. Park, J. Park and U. Jeong, *Adv. Mater.*, 2020, **32**, 1907477.
2 E. A. Widder, *Science*, 2010, **328**, 704–708.
3 A. Salih, A. Larkum, G. Cox, M. Kühl and O. Hoegh-Guldberg, *Nature*, 2000, **408**, 850–853.

4 S. H. D. Haddock, M. A. Moline and J. F. Case, *Ann. Rev. Mar. Sci.*, 2010, **2**, 443–493.
5 V. B. Meyer-Rochow, *Luminescence*, 2007, **22**, 251–265.
6 J. Tang, Y. Ren and J. Feng, *Chem. Eng. J.*, 2022, **440**, 135932.
7 R. Merindol, G. Delechiave, L. Heinen, L. H. Catalani and A. Walther, *Nat. Commun.*, 2019, **10**, 528.
8 C. Calvino, A. Guha, C. Weder and S. Schrettl, *Adv. Mater.*, 2018, **30**, 1704603.
9 G. Yin, G. Huo, M. Qi, D. Liu, L. Li, J. Zhou, X. Le, Y. Wang and T. Chen, *Adv. Funct. Mater.*, 2024, **34**, 2310043.
10 H. Liu, S. Wei, H. Qiu, M. Si, G. Lin, Z. Lei, W. Lu, L. Zhou and T. Chen, *Adv. Funct. Mater.*, 2022, **32**, 2108830.
11 J. Huang, Y. Jiang, Q. Chen, H. Xie and S. Zhou, *Nat. Commun.*, 2023, **14**, 7131.
12 R. Wang, Y. Zhang, W. Lu, B. Wu, S. Wei, S. Wu, W. Wang and T. Chen, *Angew. Chem., Int. Ed.*, 2023, **62**, e202300417.
13 X. Le, H. Shang, H. Yan, J. Zhang, W. Lu, M. Liu, L. Wang, G. Lu, Q. Xue and T. Chen, *Angew. Chem., Int. Ed.*, 2021, **60**, 3640–3646.
14 J. Ji, D. Hu, J. Yuan and Y. Wei, *Adv. Mater.*, 2020, **32**, 2004616.
15 L. Gu, H. Wu, H. Ma, W. Ye, W. Jia, H. Wang, H. Chen, N. Zhang, D. Wang, C. Qian, Z. An, W. Huang and Y. Zhao, *Nat. Commun.*, 2020, **11**, 944.
16 H. Shang, X. Le, M. Si, S. Wu, Y. Peng, F. Shan, S. Wu and T. Chen, *Chem. Eng. J.*, 2022, **429**, 132290.
17 Z. Li, P. Liu, X. Ji, J. Gong, Y. Hu, W. Wu, X. Wang, H.-Q. Peng, R. T. K. Kwok, J. W. Y. Lam, J. Lu and B. Z. Tang, *Adv. Mater.*, 2020, **32**, 1906493.
18 T. T. S. Lew, M. Park, J. Cui and M. S. Strano, *Adv. Mater.*, 2021, **33**, 2005683.
19 P. Degma, in *Water Bears: The Biology of Tardigrades*, ed. R. O. Schill, Springer International Publishing, Cham, 2018, pp. 349–369.
20 R. F. Lawrence, *J. Entomol. Soc. South. Afr.*, 1954, **17**, 167–170.
21 L. W. Victoria, H. Eloise Van, I. Nurit and V. Jean-Pol, Fluorescence in insectsPaper presented at: Proc. SPIE, 2012.
22 S. J. Stachel, S. A. Stockwell and D. L. Van Vranken, *Chem. Biol.*, 1999, **6**, 531–539.
23 L. M. Frost, D. R. Butler and B. O'Dell, *Scorpions 2001 In Memoriam Gary A. Polis*, British Arachnological Society, 2001, pp. 363–368.
24 Y. Yoshimoto, M. Tanaka, M. Miyashita, M. Abdel-Wahab, A. M. A. Megaly, Y. Nakagawa and H. Miyagawa, *J. Nat. Prod.*, 2020, **83**, 542–546.
25 W. Wu, X. Yang, H. Zhang, X. Huang, W. Zhang, M. Pan, Y. Wu, L. Zhang and K. Huang, *Polym. Chem.*, 2024, **15**, 1680–1685.
26 X. Yan, Z. Liu, Q. Zhang, J. Lopez, H. Wang, H.-C. Wu, S. Niu, H. Yan, S. Wang, T. Lei, J. Li, D. Qi, P. Huang, J. Huang, Y. Zhang, Y. Wang, G. Li, J. B. H. Tok, X. Chen and Z. Bao, *J. Am. Chem. Soc.*, 2018, **140**, 5280–5289.
27 S. Wang, X. Chen, L. Guo, S. Wang, F. Dong, H. Liu and X. Xu, *Compos. Sci. Technol.*, 2024, **248**, 110457.
28 N. Wang, X. Feng, J. Pei, Q. Cui, Y. Li, H. Liu and X. Zhang, *ACS Sustainable Chem. Eng.*, 2022, **10**, 3604–3613.
29 S. Wang and M. W. Urban, *Nat. Rev. Mater.*, 2020, **5**, 562–583.
30 S. Banerjee, B. V. Tawade and B. Améduri, *Polym. Chem.*, 2019, **10**, 1993–1997.
31 Y. Yang and M. W. Urban, *Chem. Soc. Rev.*, 2013, **42**, 7446–7467.
32 J. M. Garcia and M. L. Robertson, *Science*, 2017, **358**, 870–872.
33 C. Jehanno and H. Sardon, *Nature*, 2019, **568**, 467–468.
34 W. Li, S. Zheng, X. Zou, Y. Ren, Z. Liu, W. Peng, X. Wang, D. Liu, Z. Shen, Y. Hu, J. Guo, Z. Sun and F. Yan, *Adv. Funct. Mater.*, 2022, **32**, 2207348.
35 D. L. Taylor and M. in het Panhuis, *Adv. Mater.*, 2016, **28**, 9060–9093.
36 K. Liu, P. Han, S. Yu, X. Wu, Y. Tian, Q. Liu, J. Wang, M. Zhang and C. Zhao, *Macromolecules*, 2022, **55**, 8599–8608.
37 S. Saito, H. Ohashi, K. Nakamura, J. Otagaki, K. Nishioka, K. Nishiuchi, A. Nakamura, Y. Tsurukawa, H. Shibasaki, H. Murakami, M. Nagane, M. Okada, K. Kuramochi, K. Watashi and S. Kamisuki, *Chem. Pharm. Bull.*, 2022, **70**, 679–683.